Synergistic effects of tRNA modification defects in *Escherichia coli* K12.

Jo Marie Bacusmo[1], Jill Babor[1$], Jennifer Hu[2%,] Bo Cao[3], Stefanie Kellner[2!], Sierra Szkrybalo[1], Yifeng Yuan[1], Serena Sander[1], Paul Kuipers[1], Michael deMott[2], Hirotada Mori[4], Peter Dedon[2,3] and Valérie de Crécy-Lagard[1,5*]

[1]Microbiology and Cell Science, University of Florida, Gainesville FL 32611
[2]Department of Biological Engineering, Massachusetts Institute of Technology, Cambridge, MA 02139

[3]Antimicrobial Resistance Interdisciplinary Research Group, Singapore-MIT Alliance for Research and Technology, Singapore, Singapore.
[4]Innovation Laboratory of Systems Microbiology and Synthetic Biology, Institute of Animal Sciences, Guangdong Academy of Agricultural Sciences, Guangzhou 510640, China
[5]Genetics Institute, University of Florida, Gainesville, FL 32611

Current addresses: [$]Molecular Biology Program, Sloan-Kettering Institute, New York, NY 10065; [%]Sana Biotechnology; [!]Department of Chemistry, Ludwig-Maximilians-University Munich, Butenandtstr. 5-13, 81377, Munich, Germany

*Corresponding author
Keywords: tRNA modification, tRNA function, synthetic lethality, s^2U34

Abstract

tRNAs are the central adaptor molecule in translation and require a wide variety of post-transcriptional modifications to fulfill their functions. The model gram-negative *Escherichia coli* K-12 is one of the handfuls of bacteria where all the tRNA modifications and corresponding genes have been characterized. This work dissects epistatic relationships between tRNA modification genes in *E. coli* by conducting a synthetic lethal screen revealing 5 pairs of modifications that cannot be deleted in combination when cells are grown in rich media, and 15 pairs of modifications that lead to growth defects when deleted in combination. The *truA* gene involved in the insertion of Psi residues at positions 38 to 40 in multiple tRNAs gave the highest number of synthetic lethality phenotypes that could be complemented by the expression of the *truA* gene *in trans* and in some cases suppressed by the overexpression of target tRNAs. A pilot phenotype screen of strains lacking two tRNA modifications genes viable in rich media lead to the identification of growth conditions that exhibited poor growth. This work lays the foundation to dissect the role of modifications in tRNA quality control.

Introduction

Translation is an extremely intricate process with several key components playing integral roles in maintaining the fidelity and efficiency of the decoding machinery. At the core of this operation are tRNAs, which act as adaptor molecules bridging the nucleic acid and amino acid codes. tRNAs also participate in biological processes beyond translation such as reverse-transcription primer for some retroviruses, and amino acid donors in the biosynthesis of peptidoglycan, antimicrobial molecules, and membrane lipids (1–3). To fulfill their multiple cellular functions, tRNAs are extensively modified (4). These modifications display a wide variety of chemical complexity ranging from basic methylations to elaborate modifications like queuosine or wyeosine (5) The functions of tRNA modification are varied. They allow tRNAs to decode mRNAs accurately and efficiently (5–7), stabilize their tertiary structure (8), and act as determinants for other components of the translation apparatus such as aminoacyl-tRNA synthetase(8) or ribonuclease (9) to name a few. Further, tRNA modification profiles have been shown to respond to stress and changes in physiological conditions of the cell (10). This adaptive response allows for the translational regulation of gene expression pertinent to specific stresses or cellular demands (11, 12). It has been well established for over twenty years that in yeast RNA modifications serve as checkpoints for RNA integrity as tRNA lacking one (or more) modifications are degraded by different tRNA surveillance pathways (12–15). More recently, it was shown that the absence of tRNA modifications could also lead to degradation of bacterial tRNAs. In *Vibrio cholerae*, tRNAs lacking s^4U are rapidly degraded in stationary phase in degradosome-dependent manner (16). In *Salmonella typhimurium* LT2, the absence of Ψ38-40 in tRNA can lead to its cleavage and to the activation of a repair pathway (17).

Synthetic lethality screens have been effective in dissecting the role of tRNA modifications in tRNA quality control pathways. The first example was in yeast where a combination of 10 pairs of tRNA modification mutants were analyzed and led to the discovery of quality control tRNA degradation pathways (15, 18), The second was in *V. cholerae* where a TnSeq analysis of a *thiI* strain deficient in s^4U led to the identification of negative genetic interaction with the *truA*, *miaA* and *truA* that revealed that the degradosome targeted unmodified tRNAs (16). However, no synthetic lethal screens have, to date, focused solely on a whole set of bacterial tRNA modification genes. *Escherichia coli* is the most studied bacterial model gram-negative and numerous synthetic lethal screens have been conducted in this organism. Some screens focus on specific groups of genes such as transcription factors (19) or small RNAs (20). Other screens focused on functional areas such as DNA repair (21) or translation (22). Only 14 modification genes out of the 43 known in *E. coli* (23) were included in the latter study but no synthetic lethal pairing of tRNA modification genes were identified in this data set. To palliate the absence of systematic study, we therefore conducted a synthetic lethal screen of 29 tRNA modification genes in the model *E. coli*

Results

tRNA modification profiles of 29 tRNA modification mutants confirm expected phenotypes but does not reveal major cross-talks

All *E. coli* modification genes have now been identified (24) but a few were still missing when we performed this study, thus were excluded in our analysis (underlined in **Fig. 1A**). Further, several genes are essential (in green in **Fig. 1A**) or involved in the same pathway such as Queuosine. We chose a set of 31 genes covering 27 nucleoside modifications at 20 positions along the tRNA (in red in **Fig. 1A**) and obtained the corresponding mutants from the Keio collection (**Table S1**). Bulk tRNA was extracted and purified from 3 biological replicates of each of the *E. coli* BW2511 derivatives devoid of the 31 specific tRNA modifying genes. The tRNA modification profiles were then analyzed via mass spectrometry as described in the method section. As expected, we see a significant decrease in the levels of a given modification when the gene responsible for its synthesis is deleted (**Fig. 1B, Supplemental data S1)**: ac^4C is absent in Δ*tmcA*, cmo^5U in Δ*cmoB*, i^6A in Δ*miaA*, ms^2i^6A in Δ*miaB*, m^2A in Δ*rlmN*, m^6A in Δ*trmM*, Gm in Δ*trmH*, m^5U in Δ*trmA*, s^2C in Δ*ttcA*, s^4U in Δ*thiI*, m^6t^6A in Δ*trmO*, and Q in Δ*queG*. A significant decrease in both epoxy-Q (oQ) and Q is observed in Δ*tgt* because Tgt is responsible for the transfer of $preQ_1$ (precursor to both oQ and Q).

We also see expected trends in cases where several genes are responsible for one modification as in the case of dihydrouridine (D) and Cm/Um. Most of the D modifications in tRNA are contributed by *dusA* and *dusB* while a smaller subset is modified by *dusC* (25). Our results reflect this as we observe a 5-fold decrease in modification levels when *dusA* and *dusB* are deleted compared to when only *dusC* is deleted (**Supplemental data S1**). Modification of 2'-O-methylated cytidine (C_m32) or 2'-O-methylated uridine (U_m32) at position 32 in tRNA is

catalyzed by *trmJ* (to $tRNA^{fMet}_{CAU}$, $tRNA^{Trp}_{CCA}$, $tRNA^{Gln}_{CUG}$, $tRNA^{Gln}_{UUG}$, $tRNA^{Ser}_{UGA}$)(26) and *trmL* (to $tRNA^{Leu}_{CAA}$ and $tRNA^{Leu}_{UAA}$)(27). Our results reflect the difference in the population of target tRNAs between the two genes where about a 16-fold decrease in Cm/Um modification levels are observed when *trmJ* is deleted compared to when *trmL* is deleted (**Supplemental data S1**).

We also observe accumulation of a precursor when we delete the gene responsible for the downstream reaction in the pathway as in the cases of Δ*miaB*, Δ*queG*, and Δ*mnmG* (**Fig.1B**). MiaB catalyzes the reaction that converts i^6A into ms^2i^6A(28), thus an accumulation of i^6A is observed in its absence. Similarly, an accumulation of oQ is observed in the Δ*queG* strain, as the missing enzyme catalyzes the conversion of oQ to Q (29). Finally, an accumulation of s^2U is observed in the Δ*mnmG* strain as the MnmG-MnmE complex converts s^2U into either $cmnm^5s^2U$ or nm^5s^2U(30). Altogether, these observations validate our data set on each of the tRNA modification profiles.

Previous studies reported that i^6A37 or ms^2i^6A37 stimulate U_m34 and C_m34 formation in *E. coli* $tRNA^{Leu}_{UAA}$ and $tRNA^{Leu}_{CAA}$ (31). We did not observe any reduction in Cm levels in the *miaA* mutant but as we stated above, this could be because TrmJ-dependent methylations are still present in this strain.

One unexpected result was the disappearance of $cmnm^5s^2U$ in the *thiI* mutant (**Fig. 1B, Supplemental data S1**). $Cmnm^5s^2U$ is found in $tRNA^{Gln}_{UUG}$ at position 34. Its synthesis requires three enzymes: MnmEG for the formation of $cmnm^5U$ and MnmA for the thiolation step(32). ThiI is the enzyme involved in the synthesis of s^4U at position 8 found in many tRNAs including $tRNA^{Gln}_{UUG}$ (33). The cysteine desulfurase, IscS, provides the sulfur moiety to both ThiI and MnmA (34). Levels of nm^5s^2U, another modification dependent on the *mnmA* pathway

found in $tRNA^{Lys}_{UUU}$ and $tRNA^{Gln}_{UUG}$ were not affected by the absence of *thiI*. $tRNA^{Lys}_{UUU}$ does not contain s^4U while $tRNA^{Gln}_{UUG}$ does (33).. No obvious explanation for this observation could be proposed. If there is competition for the sulfur source, then one would expect that the absence of ThiI would lead to increased and not decreased s^2U levels. If s^4U is determinant for MnmA then only $tRNA^{Gln}_{UUG}$ should be affected and there should be a reduction not an elimination of $cmnm^5s^2U$.

Evaluation of epistatic relationships between tRNA modifying genes reveal a subset of genes with higher propensity towards synthetic lethality

To explore epistatic relationships between tRNA modifying genes, a synthetic lethal screen was conducted. A pair-wise deletion matrix of 29 tRNA modifying genes covering 25 different modifications was generated via P1 transduction and evaluated based on the number of transductants obtained relative to the wild-type control. Two sets of deletion strains were used as donors and recipients for the P1 transduction: one set contained chloramphenicol resistance cassette (Cam^R) inserted in the place of the deleted tRNA modification gene, while the second set contained a kanamycin resistance cassette (Kan^R, strains were taken from the Keio collection). The list of the strains used is given in **Table S1**. Transductions were performed in both directions selecting for transductants resistant to both Chloramphenicol and Kanamycin. All mutant combinations giving rise to no transductants, less transductants, or transductants with smaller colony sizes were repeated independently (**Supplemental Data S2A**). We also verified that none of the pairs that gave growth phenotypes were located within co-transduction distance as this would lead to artifacts (**Fig. S1**) The synthetic lethal screen showed that 95% (357 pairs) of the tested combination of deletions of tRNA modification genes gave WT looking colonies on

LB at 37ºC, while 4% (15 pairs) gave fewer transductants or transductants with smaller colony sizes and 1% (5 pairs) resulted in synthetic lethality (**Fig. 2**). Seven genes appeared in synthetic lethal pairs: Δ*truA*, Δ*mnmA*, Δ*rlmN*, *ΔrluA*, Δ*miaA*, Δ*truD*, and Δ*trmJ*. Out of the five synthetic lethal pairs, four encode enzymes modify the Anticodon Stem Loop (ASL) *(ΔrlmNΔmiaA*, *ΔtruAΔmnmA*, *ΔtruAΔrlmN*, *ΔtrmJΔtruA*) while one pair encodes enzyme that has modification the D-arm and the ASL respectively *(ΔtruDΔrluA*) (**Fig. S2**).The MnmA/MnmG synthetic lethality had been previously reported in *S. enterica* LT2 (35)and was reproduced here in *E. coli*.

The highest percentage of negative epistasis was observed when transducing any of the *dusB*, *mnmA*, *mnmC*, *mnmG*, *mnmH*, *rlmN*, *trmA* or *trmJ* deletion alleles into the Δ*truA* strain with a variety of phenotypes (small colonies, fewer or no colonies). As all the attempts to obtain a Δ*truA*Δ*mnmA* clones failed, we studied this synthetic lethality phenotype further. The Δ*truA::*Kan^R strain was transformed with a pBAD24*truA* derivative allowing controlled expression of *truA in trans*. We then transduced the Δ*mnmA*::Cam^R allele into the trans Δ*truA*::Kan^R pBAD24*truA* strain as well as in the same strain transformed with the control pBAD24 vector and selected for transductants in the presence and absence of 0.02% arabinose. Transductants were only obtained when *truA* was expressed *in trans* and adding inducer led to more transductants. (**Fig. 3**). Similarly, expressing the *truA* gene i*n trans* complemented the epistatic growth defects fully (for *dusB*, *mnmH* and *trmJ*) or partially (for *mnmC*. *trmA* and *rlmN*) (**Fig. S3**). The only tRNA that requires MnmA and TruA to be fully modified is $tRNA^{Gln}_{UUG}$ (**Fig. 4**) and indeed, expressing this tRNA in trans partially suppressed the Δ*truA*Δ*mnmA* synthetic lethality (**Fig. 3**).

The absence of unique tRNA modifications does not drastically influence tRNA levels in *E. coli* K12

One possible cause for observing synthetic lethality phenotypes when combining tRNA modification genes is that the tRNAs lacking the two modifications are degraded by RNase as recently seen in *Vibrio* or *Salmonella* (36, 37). Using AQRNA-seq**,** a tRNA-seq method that can measure absolute levels (38), we quantified levels of all *E. coli* tRNAs in cells grown to mid-log phase (OD A600nm of ~0.5) in 10 of the 16 mutant strains that led to synthetic lethality phenotypes in certain combinations (**Fig. S4** and **Supplemental data S3**)

We found that the levels of 11 tRNA decreased significantly in tRNA modifications mutants (Supplemental data S3F), 9 of those were modified by the corresponding enzymes (**Supplemental data S3F**) but matched with the synthetic lethal combinations.

Synthetic lethal screens lead to the discovery of condition-dependent synthetic lethality

As discussed above, deletion of *rlmN*, *mnmA*, *trmJ* or *truA* resulted in synthetic lethal combinations with several other tRNA modification mutants (**Fig. 2**). These four genes encode enzymes that modify a common substrate: $tRNA^{Gln}_{UUG}$ (**Fig. 4A**) but did not lead to any growth defects when deleted in pairwise combinations in the initial screen performed on LB (**Fig. 2**). To study these strains further, we generated the 6 pairwise deletion strains through P1 transductions (**Table S1**). We tested the fitness of the double deletion pairs by determining the growth rate in LB at 37°C (**Fig. S5**). The Δ*rlmNΔmnmA* and Δ*trmJΔmnmA* strains showed a slight growth defect, with Δ*rlmNΔmnmA* exhibiting an increased lag phase compared to Δ*rlmN* and Δ*mnmA* strains (**Fig. S5**). We then conducted a screen to determine whether growth of the Δ*rlmNΔmnmA* strain could be affected under specific growth conditions by varying the carbon source (glucose,

xylose, acetate, glycerol, and succinate) and the incubation temperature (30°C, 37°C, or 42°C). We found that Δ*rlmNΔmnmA* mutant showed a slight growth defect when cultured on acetate and xylose containing media at 37°C (**Fig. S5**). All strains carrying the *mnmA* deletion failed to grow on acetate at high temperature but only the Δ*rlmNΔmnmA* strain failed to grow on xylose at 42°C (**Fig. 5**). $tRNA^{Gln}_{UUG}$ is the only tRNA modified by s^2U and m^2A37 (**Fig. 4**). We therefore tested whether overexpression of $tRNA^{Gln}_{UUG}$ could suppress the temperature sensitivity (TS) of the Δ*rlmNΔmnmA* strain when grown with xylose as carbon source. Indeed, we found that $tRNA^{Gln}_{UUG}$ suppresses the TS phenotype in xylose but not $tRNA^{Gln}_{CUG}$. (**Fig. S5C**).

It has been previously reported that excess xylose can lead to increased production of methylglyoxal (39). The two methylglyoxal detoxification pathway genes *gloA* and *gloB* preferentially use the UUG codons decoded by tRNA Gln1 (**Supplemental data S4**). When grown in M9-salts supplemented with 0.4% glycerol and 0.5mM methyglyoxal, *rlmN mnmA* shows a growth defect compared to WT and the single knockouts.

Discussion

By systematically constructing all pairwise combinations of 29 *E. coli* tRNA modifications genes, we identified specific phenotypes caused by absence of two tRNA modifications genes (Fig. 2). Twenty cases of negative epistasis were identified and 8 of those involve *truA*. Three of 5 synthetic lethal pairs (*truA*/r*lmN*, *rlmM*/*miaA* and *trmJ*/*truA*) had showed negative genetic interaction scores in the synthetic lethality screens that focuses on translation genes from the Emili laboratory but these were under their high-confidence cut-off (22). Also, several tRNA modification genes including *mnmA* were not present in the initial

target list. Hence, our results reinforce the value of orthogonal approaches to measure essentiality as we use P1 transduction efficiency, and the Emili group study used colony size.

The roles of specific tRNA modifications seem to vary greatly both with the organism, and the growth conditions. We did not observe in *E. coli* the synthetic lethality of *thiI* with *miaA*, *truB* and *trmA* observed in *V. cholerae* (16). We did see that the combination of *thiI* and *mnmG* deletions was detrimental (**Fig. 2**). Similarly, in Salmonella the absence of Ψ39-40 in a *truA* mutant leads to the accumulation of tRNA halves but this is not the case in *E. coli* as already reported by the Wolin laboratory (17) (**Supplemental data S3**). Growth conditions are also critical to reveal the physiological roles of tRNA modifications. For example, the degradation of tRNATyr by the degradosome in the absence of ThiI in *V. cholerae* is mainly observed in stationary phase (16). In the same organism the growth defects of the *thiI miaA*, *thiI truB* and *thiI trmA* strains is more pronounced at 37ºC compared to 25ºC (16). In our study, the growth defects of the *rlmN mnmA* strain were dependent on both the carbon source and the temperature (**Fig. 5**). Hence to fully explore the physiological roles of tRNA modification will require the use of genome wide TnSeq screens using tRNA modification deletion strains as starting points as the technology to perform such screens has recently become available (40). These whole genome screens could also identify interactions between tRNA modifications genes and other genes related or not to translation. For example, targeted studies have shown that deleting *truA* or *iscS* is synthetic lethal in combination with the Δ*rnhAB* deletion that is deficient in RnaseH revealing that translation efficiency affects DNA replication (41).

The presence of Ψ39-40 in the ASL dependent on TruA is emerging as key quality control marker for tRNA integrity in different organisms but possibly through different mechanisms. We also found that in *E. coli* K12 tRNAGln1 seems to be particularly dependent on

tRNA modifications for stability and further studies are required to identify the players involved even if it is highly probable that the degradosome is involved. Finally, this work reinforces the power of using epistatic interactions screens in general to discover novel molecular mechanisms even in a very well-studied organism like *E. coli* K12.

Methods

Bioinformatics

Information on *E. coli* genes was extracted from EcoCyc(42) and the resources of NCBI including Pubmed (43). Codon usage was performed using the Codon UTilization tool (CUT) tool(44)

Bacterial strains, plasmids and media

Luria-Bertani (LB) broth and agar (tryptone 10 g/L, yeast extract 5 g/L, sodium chloride 10 g/L, Fisher Scientific BP1426-2 and BP1425-2) were routinely used for growth of *E. coli* cells at 37°C from frozen stocks. M9 minimal medium (12.8 g/L $Na_2HPO_4 \cdot 7H_2O$, 3.0 g/L KH_2PO_4, 0.5 g/L NaCl, 1.0 g/L NH_4Cl, 2.0 mM $MgSO_4$, 0.1 mM $CaCl_2$) was used with 0.4% glucose, xylose, acetate, glycerol, or succinate as carbon sources. When required, 50 µg/mL of kanamycin (Kan), 100 µg/mL Ampicillin (Amp), 20 µg/mL of chloramphenicol (Cm), 2.5 µM-1mM Isopropyl β-D-1-thiogalactopyranoside (IPTG), methylglyoxal (0.1 or 0.5mM) or Arabinose (0.02%) were added to the medium. Bacterial growth was followed in a Bioscreen C (Growth Curve, USA) by measuring OD at A(600nm) over a period of 18-24 hours.

The bacterial strains used in this study are listed **Table S1**. Most are from the Keio collection (45) and from a set of Hfr strains containing a single deletion of tRNA modifying genes replaced by Cm^R cassette (H. Mori) (46). Markerless deletions strains were generated by FLP mediated excision of the Kan^R cassette through pCP20 (47) for a subset of Keio collections strains. Plasmid transformations were performed by electroporation using manufacturer's settings (Bio-Rad Micropulser). All strains carrying two tRNA modification alleles were

constructed by P1 transduction as described below. All the strains were validated for the correct genotype using the primers listed on Supplementary **Table S2.**

The fragments encoding tRNAgln1^{UUG} and tRNAgln2^{CUG} were subcloned from pSADgln1,2 (48) into the EcoRI and PstI sites in pTrc99A yielding pJMB23(tRNAgln1) and pJMB24(tRNAgln2). pTrc99A, pJMB23, and pJMB24 were transformed into wildtype, Δ*mnmA::cat*Δ*rlmN::kan*, Δ*rlmN::cat*Δ*mnmA::kan*, and Δ*truA::kan* through electroporation. *truA* was amplified by PCR using *E. coli* BW25113 genomic DNA as template using a primer pair bearing 5′-EcoRI and 3'-SalI sites (Table S2). The PCR product was digested with EcoRI and SalI (NEB) and ligated (NEB T4 DNA ligase) into the corresponding sites in pBAD24 yielding pBAD::truA. pBAD24 and pBAD::truA were transformed into wildtype and Δ*truA::kan* through electroporation.

Synthetic lethality analysis by P1 Phage Transduction

P1vir phage (49) donor lysates were prepared from single deletion strains containing a Chloramphenicol resistance cassette (Cm^R) in place of the deleted gene (46). The single deletion strains from the Keio collection (45) containing a Kanamycin resistance cassette (Kan^R) served as the recipient. Donor Lysates were prepared as previously described (50). Briefly, donor strains were grown in P1-LB (LB supplemented with 5 mM $CaCl_2$, 0.1% glucose, and 12.5mM of $MgCl_2$) to an OD of 0.6, to which 40 µL of P1vir phage was added. Infection was allowed to proceed for 4 hours until cell debris was visible. The mixture was then centrifuged for 15 minutes at 4,000 rpm to separate the cell debris. The supernatant was passed through a 0.2 µM filter to remove any trace cell debris and residual bacteria. 200 µL chloroform was added to prevent bacterial growth in the lysate. Recipient strains were grown in P1-LB to an OD of 0.6.

One mL was transferred into a 2 mL centrifuge tube and centrifuged at 13,000 rpm for 1 minute. Cell pellets were resuspended in 100 µL P1-LB, to which 20 µL of the donor lysate was added. Transfection was allowed to proceed for 15 minutes with constant orbital shaking at 180 rpm. Reaction was terminated by adding 200 µL of 1M Sodium Citrate pH 5.5 and 1 mL LB. Transductants were allowed to recover for 2 hours in 37°C with shaking. Reaction was centrifuged at 13,000 rpm and the pellet was resuspended in 150 µL LB-Citrate (LB supplemented with 100 mM Sodium Citrate pH 5.5) and plated on LB-agar plates supplemented with 50 µg/mL Kanamycin and 25 µg/mL Chloramphenicol for selection. Plates were incubated at 37°C for 16-20 hours. The transduction efficiency was assessed by quantifying colony-forming units (CFU) comparing to a wildtype (WT) recipient. We used the following scale to categorize transduction efficiencies: 1-10 colonies – defective, zero colonies – lethal, small colonies. A second round of P1 transductions was performed independently to verify the 31 pairs categorized as synthetic lethal pairs from the initial round (**Supplemental Data S2**).

tRNA purification

E. coli cultures (10 mL) grown to A_{600} ~0.6 were harvested by centrifugation 4 °C for 10 min at 3700 xg. Pellets were resuspended in 1 mL of Trizol (Life Technologies) and agitated on a rocking shaker for 2-4 h. Small RNA was extracted using a Purelink miRNA Isolation kit (Invitrogen) and RNA eluted in 50 µL of RNase-free water. Following RNA quantification by Nanodrop, samples with A_{260}/A_{230} ratios <1.6 were cleaned using an RNA Clean and Concentrator Kit (Norgen Biotek).

Mass Spectrometry Analysis of tRNA

RNA in each sample (1.8 µg) was hydrolyzed in a 30 µL digestion reaction containing 2.49 U benzonase, 3 U CIAP (calf intestinal alkaline phosphatase), 0.07 U PDE I (phosphodiesterase I), 0.1 mM deferoxamine (antioxidant), 0.1 mM butylated hydroxytoluene (antioxidant), 3 ng coformycin (adenosine deaminase inhibitor), 25 nM [$^{15}N_5$]-2'-deoxyadenosine (internal standard), 2.5 mM $MgCl_2$ and 5 mM Tris-HCl buffer pH 8.0. The digestion mixture was incubated at 37 °C for 6 h. After digestion, all samples were loaded into sample vials containing an Agilent sample vial insert and analyzed by chromatography-coupled triple-quadrupole mass spectrometry (LC-MS/MS). For each duplicate sample, 600 ng of hydrolysate was injected twice as technical replicates on a Waters Acuity BEH C18 column (50 × 2.1 mm inner diameter, 1.7 µm particle size) eluted with the following buffer gradient of Buffer A (0.02% formic acid) and Buffer B (0.02% formic acid in 70% acetonitrile) was used for elution of ribonucleosides at 0.3 mL/min according the time frame given **Table S3**. The HPLC column was coupled to an Agilent 1290 HPLC system and an Agilent 6495 Triple Quadrupole LC/MS spectrometer and eluted at a flow rate of 0.3 mL/min and 25 °C, with an electrospray ionization source in positive mode with the following parameters: drying gas temperature, 200 °C; gas flow, 11 L/min; nebulizer, 20 psi; sheath gas temperature, 300 °C; sheath gas flow, 12 L/min; capillary voltage, 3000 V; nozzle voltage, 0 V. The first and third quadrupoles (Q1 and Q3) were fixed to unit resolution and the modifications were quantified by pre-determined molecular transitions. The dwell time was 500 ms, the fragmentor voltage was 166 V, and the cell accelerator voltage was 5 V for each nucleoside. Multiple reaction monitoring (MRM) mode was used for detecting product ions derived from precursor ions for the ribonucleosides, with instrument parameters including the collision energy (CE) optimized for maximal sensitivity for

the modification. Synthetic standards (except for oQ) were used to define HPLC retention times of RNA modifications. The retention time, *m/z* of the transmitted parent ion, and *m/z* of the monitored product ion for each ribonucleoside are detailed in **Table S4**. All MRM peak integrations were manually checked.

Determination of absolute tRNA levels by AQRNA-seq

AQRNA-seq library preparation. AQRNA-seq analysis of tRNA isoacceptors was performed as described in detail elsewhere(38). Briefly, purified small RNA (50 ng) was mixed with an 80-mer spike-in RNA oligonucleotide internal standard (DNA and RNA oligonucleotide sequences in **Table S5**).5 The mixture was dephosphorylated shrimp alkaline phosphatase (rSAP, NEB) in NEB T4 RNA ligase buffer at 37 °C for 30 min, followed by heat inactivation at 65 °C for 5 min and cooling on ice. Linker 1 ligation was performed by adding Linker 1 (100 pmol/ul; **Table S5**), ATP (10 mM, NEB), T4 RNA ligase buffer (NEB), T4 RNA ligase 1 (30U/ul, NEB), water and PEG8000 (NEB) to the reaction mixture. Following incubation at 25 °C for 2 h and then at 16 °C overnight, the ligation product was purified using the Zymo Oligo Clean & Concentrator kit (Zymo Research, D4060). The sample was eluted in water and kept on ice prior to Bioanalyzer analysis (Agilent, small RNA kit) or used directly in the demethylation step. Next, the DNA adenylated oligonucleotide adenylate intermediate was de-adenylated (RNA sample, NEB Buffer 2, and 5'-deadenylase (NEB); incubation at 30 °C for 1 h) and removed together with unused Linker 1 in a 30 min incubation with exonuclease RecJ (NEB). The reaction was stopped by heating at 65 °C for 20 min and products purified using a DyEx spin column (Qiagen). Reverse transcription was performed by mixing purified RNA with RT-primer (2 pmol/ µl) and dNTPs (10 mM each) and heating to 80 °C for 2 min, followed by cooling on ice.

PrimeScript Buffer (Clontech), RNase Inhibitor (NEB), and PrimeScript Reverse Transcriptase (Clontech) were added with incubation at 50 °C for 2 h followed by enzyme inactivation at 70 °C for 15 min. The RNA strand was removed by adding NaOH (5 M) with incubation at 90 °C for 3 min, followed by neutralization with HCl (5M) and cDNA purification using the Zymo Oligo Clean & Concentrator kit (Zymo Research). The sample was eluted with water and vacuum concentrated to 5 ul. The purified cDNA was ligated to Linker 2 (**Table S5**) with T4 DNA Ligase Buffer (NEB), ATP (NEB), T4 DNA ligase (NEB), and PEG8000 (NEB) at 16 °C overnight. Ligated product was purified using the Zymo Oligo Clean & Concentrator kit and eluted in 16 µl of water. Excess Linker 2 and adenylated linker products were removed by RecJ and the reaction was stopped through heat inactivation at 65 °C for 20 min. Purified cDNA was then amplified by PCR in seqAMP DNA polymerase buffer (Clontech) with PCR primer F and R with unique sequencing barcodes (**Table S5**), seqAMP DNA polymerase (Clontech), and water. PCR was performed with an annealing temperature of 58 °C and 13 reaction cycles followed by agarose gel resolution and extraction using a standard gel purification kit (QIAquick Gel Extraction Kit, Qiagen). The gel-extracted samples were mixed for multiplexing and submitted for Illumina NextSeq sequencing.

AQRNA-seq data processing. Illumina sequencing reads were assessed using a quality control pipeline and the data subsequently processed using a workflow described in detail elsewhere(38). Briefly, adapter sequences were removed from forward and reverse reads using fastxtoolkit (v0.013). Sequences were blasted against a reference library (including the 80-mer internal standard) using blast (v2.6.0) with the parameters: blast -perc identity 90 -word_size 9 -dust no -soft_masking false. Sequences corresponding to duplicate tRNA genes and tRNA pseudogenes

were removed to eliminate redundant entries and reduce the incidence of ambiguous or false positive matches. The terminal (3') CCA sequence was added to tRNA sequences where it is not genomically encoded. For each tRNA and control sample, forward and reverse reads were merged by integrating their start and end positions to generate new start and end positions that reflect their combined coverage. Using the python script cull.py, multiple alignments were reduced by ranking all the alignments for a given read by their e-value and retaining only the alignment with the lowest e-value, retaining forward and reverse reads that matched the same target. Uniquely mapped reads were then tabulated and counted.

Funding

This work was funded by the National Institute of General Medical Sciences (NIGMS) grant GM70641, by the National Science Foundation (NSF) MCB1412379, by the National Research Foundation of Singapore under the Singapore-MIT Alliance for Research.

Acknowledgments

We thank Thomas Begley (University at Albany) for running the CUT analysis on the *E. coli* genome and William McClain for sharing the pSADgln1,2 plasmid.

Figure Legends

Figure 1. tRNA modifications proteins in *E. coli* K12 strain MG1655 and validation by LC_MS of mutants analyzed in study. (A) Positions of the modifications and associated proteins and genes (locus tag are in parentheses). Modifications that were targeted are in red. Those inserted by essential genes are in green. Genes that were not identified at the time of the study are underlined. *Also modifies rRNA. (B) tRNA modification profiles in 31 different tRNA modification deficient strains. The Keio collection tRNA modification mutant strain genotypes are listed in **Table S1**. Modification abbreviations according to Modomics (http://genesilico.pl/modomics/modifications). Data are presented as log2 values of fold-change relative to wild-type *E. coli* subjected to hierarchical clustering analysis. "X" denotes analyses for which no detectable signals were obtained for the modification.

Figure 2. Synthetic lethality screen of 29 tRNA modification genes. All the mutant combinations that intersect with white boxes gave rise to transductant numbers equivalent to transducing the WT strain. The combinations that gave rise to growth phenotypes are noted by black (no transductant), medium grey (fewer transductants) or light grey (small colonies and fewer transductants) boxes. The mutant combinations giving rise to phenotypes on the initial screened were confirmed individually (**Supplemental data S2A**).

Figure 3. The synthetic lethality phenotype of the *truA* and *mnmA* genes is complemented by expressing the *truA* gene in trans suppressed by overexpressing tRNA-Gln1. P1 transduction efficiency when selecting for the insertion of the *mnmA*::Cam^R allele into the WT or

truA::Kan^R strains or into derivatives transformed with a control plasmid (pBAD24) or plasmids expressing the *truA* gene (p*truA*), or tRNA genes [tRNA-Gln1 (pGln1) or tRNA-Gln2 (pGln2)]. The selection for transductants was performed on LB plates all supplemented with kanamycin and chloramphenicol with and some with arabinose (0.02%) or IPTG. The numbers of transductants were counted after 24h incubation at 37ºC.

Figure 4. The tRNA decoding capacities and ASL modifications of *E. coli*. Letters from inside out indicate the codon's first, second, and third position (5′- to 3′- end) as the subscripts indicate. The circles outside of the wheel connected or not by a line represent one tRNA species. A filled circle indicates the capacity of that tRNA to base pair with the indicated codon by Watson-Crick pairing. An open (white) circle suggests base pairing by the wobble hypothesis (51). The base at position 34 of the anticodon and the anticodon stem loop (ASL) modifications in positions 32 to 40 are shown next to each tRNA circle. Amino acids that are decoded by a single tRNA are highlighted in red. Data are compiled from (33, 51–53). Discrepancies among references are shown in parentheses, suggesting partial modifications or modifications at certain conditions.

Figure 5. Growth phenotypes of the *rlmN mnmA* strain. (A) Growth of the WT, *rlmN*, *mnmA* and *rlmN mnmA* strains at 42ºC in M9 supplemented with glucose (0.4%), acetate (0.4%) or xylose (0.4%) as carbon source; (B) Growth of the WT, *rlmN*, *mnmA* and *rlmN mnmA* strains at 37ºC in M9 with glycerol as carbon source and with or without methylglyoxal.

55

56

References:

1. Chery M, Drouard L. 2023. Plant tRNA functions beyond their major role in translation. J Exp Bot 74:2352–2363.

2. Marquet R, Isel C, Ehresmann C, Ehresmann B. 1995. tRNAs as primer of reverse transcriptases. Biochimie 77:113–124.

3. Raina M, Ibba M. 2014. TRNAs as regulators of biological processes. Front Genet 5:92747.

4. Yared MJ, Marcelot A, Barraud P. 2024. Beyond the anticodon: tRNA core modifications and their impact on structure, translation and stress adaptation. Genes (Basel) 15:374.

5. El Yacoubi B, Bailly M, De Crécy-Lagard V. 2012. Biosynthesis and function of posttranscriptional modifications of transfer RNAs. Annu Rev Genet 46:69–95.

6. Pollo-Oliveira L, de Crécy-Lagard V. 2019. Can protein expression be regulated by modulation of tRNA Modification profiles? Biochemistry 58:355–362.

7. Grosjean H, de Crécy-Lagard V, Marck C. 2010. Deciphering synonymous codons in the three domains of life: Co-evolution with specific tRNA modification enzymes. FEBS Lett 584:252.

8. Madore E, Florentz C, Giege R, Sekine S, Yokoyama S, Lapointe J. 1999. Effect of modified nucleotides on *Escherichia coli* tRNAGlu structure and on its aminoacylation by glutamyl-tRNA synthetase. Predominant and distinct roles of the mnm^5 and s^2 modifications of U34. Eur J Biochem 266:1128–35.

9. Bacusmo JM, Orsini SS, Hu J, DeMott M, Thiaville PC, Elfarash A, Paulines MJ, Rojas-Benítez D, Meineke B, Deutsch C, Iwata-Reuyl D, Limbach PA, Dedon PC, Rice KC, Shuman S, de Crécy-Lagard V de. 2018. The ^{t6}A modification acts as a positive determinant for the anticodon nuclease PrrC, and is distinctively nonessential in *Streptococcus mutans*. RNA Biol 15:508.

10. Huber SM, Leonardi A, Dedon PC, Begley TJ. 2019. The versatile roles of the tRNA epitranscriptome during cellular responses to toxic exposures and environmental stress. toxics 7:17.

11. Endres L, Dedon PC, Begley TJ. 2015. Codon-biased translation can be regulated by wobble-base tRNA modification systems during cellular stress responses. RNA Biol 12:603–614.

12. Duechler M, Leszczyńska G, Sochacka E, Nawrot B. 2016. Nucleoside modifications in the regulation of gene expression: focus on tRNA. Cell Mol Life Sci 73:3075–3095.

13. Phizicky EM, Hopper AK. 2023. The life and times of a tRNA. RNA 29:898–957.

14. De Zoysa T, Hauke AC, Iyer NR, Marcus E, Ostrowski SM, Stegemann F, Ermolenko DN, Fay JC, Phizicky EM. 2024. A connection between the ribosome and two *S. pombe* tRNA modification mutants subject to rapid tRNA decay. PLoS Genet 20:e1011146.

15. Alexandrov A, Chernyakov I, Gu W, Hiley SL, Hughes TR, Grayhack EJ, Phizicky EM. 2006. Rapid tRNA decay can result from lack of nonessential modifications. Mol Cell 21:87–96.

16. Kimura S, Waldor MK. 2019. The RNA degradosome promotes tRNA quality control through clearance of hypomodified tRNA. Proc Natl Acad Sci U S A 116:1394–1403.

17. Hughes KJ, Chen X, Burroughs AM, Aravind L, Wolin SL. 2020. An RNA repair operon regulated by damaged tRNAs. Cell Rep 33:108527.

18. de Zoysa T, Phizicky EM. 2020. Hypomodified tRNA in evolutionarily distant yeasts can trigger rapid tRNA decay to activate the general amino acid control response, but with different consequences. PLoS Genet 16:e1008893.

19. Gagarinova A, Hosseinnia A, Rahmatbakhsh M, Istace Z, Phanse S, Moutaoufik MT, Zilocchi M, Zhang Q, Aoki H, Jessulat M, Kim S, Aly KA, Babu M. 2022. Auxotrophic and prototrophic conditional genetic networks reveal the rewiring of transcription factors in *Escherichia coli*. Nature Comm 2022 13:1 13:1–16.

20. Das S, Forrest J, Kuzminov A. 2023. Synthetic lethal mutants in *Escherichia coli* define pathways necessary for survival with RNase H deficiency. J Bacteriol 205.

21. Kumar A, Beloglazova N, Bundalovic-Torma C, Phanse S, Deineko V, Gagarinova A, Musso G, Vlasblom J, Lemak S, Hooshyar M, Minic Z, Wagih O, Mosca R, Aloy P, Golshani A, Parkinson J, Emili A, Yakunin AF, Babu M. 2016. Conditional epistatic interaction maps reveal global functional rewiring of genome integrity pathways in *Escherichia coli*. Cell Rep 14:648–661.

22. Gagarinova A, Stewart G, Samanfar B, Phanse S, White CA, Aoki H, Deineko V, Beloglazova N, Yakunin AF, Golshani A, Brown ED, Babu M, Emili A. 2016. Systematic genetic screens reveal the dynamic global functional organization of the bacterial translation machinery. Cell Rep 17:904–916.

23. de Crécy-Lagard V, Jaroch M. 2021. Functions of bacterial tRNA modifications: from ubiquity to diversity. Trends Microbiol 29:41–53.

24. Wang J, Toffano-Nioche C, Lorieux F, Gautheret D, Lehmann J. 2021. Accurate characterization of *Escherichia coli* tRNA modifications with a simple method of deep-sequencing library preparation. RNA Biol 18:33.

25. Bishop AC, Xu J, Johnson RC, Schimmel P, De Crécy-Lagard V. 2002. Identification of the tRNA-dihydrouridine synthase family. J Biol Chem 277:25090–25095.

26. Purta E, van Vliet F, Tkaczuk KL, Dunin-Horkawicz S, Mori H, Droogmans L, Bujnicki JM. 2006. The *yfhQ* gene of *Escherichia coli* encodes a tRNA:Cm32/Um32 methyltransferase. BMC Mol Biol 7:23.

27. Benítez-Páez A, Villarroya M, Douthwaite S, Gabaldón T, Armengod ME. 2010. YibK is the 2'-O-methyltransferase TrmL that modifies the wobble nucleotide in *Escherichia coli* tRNALeu isoacceptors. RNA 16:2131–2143.

28. Esberg B, Leung HC, Tsui HC, Björk GR, Winkler ME, Bjork GR, Winkler ME. 1999. Identification of the *miaB* gene, involved in methylthiolation of isopentenylated A37 derivatives in the tRNA of *Salmonella typhimurium* and *Escherichia coli*. J Bacteriol 181:7256–65.

29. Miles ZD, McCarty RM, Molnar G, Bandarian V. 2011. Discovery of epoxyqueuosine (oQ) reductase reveals parallels between halorespiration and tRNA modification. Proc Natl Acad Sci U S A 108:7368–7372.

30. Armengod M-E, Moukadiri I, Prado S, Ruiz-Partida R, Benítez-Páez A, Villarroya M, Lomas R, Garzón MJ, Martínez-Zamora A, Meseguer S, Navarro-González C. 2012. Enzymology of tRNA modification in the bacterial MnmEG pathway. Biochimie 94:1510–1520.

31. Han L, Phizicky EM. 2018. A rationale for tRNA modification circuits in the anticodon loop. RNA 24:1277.

32. Armengod ME, Meseguer S, Villarroya M, Prado S, Moukadiri I, Ruiz-Partida R, Garzón MJ, Navarro-González C, Martínez-Zamora A. 2014. Modification of the wobble uridine in bacterial and mitochondrial tRNAs reading NNA/NNG triplets of 2-codon boxes. RNA Biol 11:1495–1507.

33. Boccaletto P, MacHnicka MA, Purta E, Pitkowski P, Baginski B, Wirecki TK, de Crécy-Lagard V, Ross R, Limbach PA, Kotter A, Helm M, Bujnicki JM. 2018. MODOMICS: A database of RNA modification pathways. 2017 update. Nucleic Acids Res 46:D303–D307.

34. Lauhon CT. 2002. Requirement for IscS in biosynthesis of all thionucleosides in *Escherichia coli*. J Bacteriol 184:6820–9.

35. Nilsson K, Jäger G, Rk GRB. 2017. An unmodified wobble uridine in tRNAs specific for Glutamine, Lysine, and Glutamic acid from *Salmonella enterica* Serovar Typhimurium results in nonviability-Due to increased missense errors? PLoS One 12:e0175092.

36. Kimura S, Waldor MK. 2019. The RNA degradosome promotes tRNA quality control through clearance of hypomodified tRNA. Proc Natl Acad Sci U S A 116:1394–1403.

37. Schultz SK, Kothe U. 2024. RNA modifying enzymes shape tRNA biogenesis and function. J Biol Chem 300:107488.

38. Hu JF, Yim D, Ma D, Huber SM, Davis N, Bacusmo JM, Vermeulen S, Zhou J, Begley TJ, DeMott MS, Levine SS, de Crécy-Lagard V, Dedon PC, Cao B. 2021. Quantitative mapping of the cellular small RNA landscape with AQRNA-seq. Nat Biotechnol 39:978–988.

39. Ackerman RS, Cozzarelli NR, Epstein W. 1974. Accumulation of Toxic Concentrations of Methylglyoxal by Wild-Type *Escherichia coli* K-12. J Bacteriol 119:357.

40. Jana B, Liu X, Dénéréaz J, Park H, Leshchiner D, Liu B, Gallay C, Zhu J, Veening J-W, van Opijnen T. 2024. CRISPRi–TnSeq maps genome-wide interactions between essential and non-essential genes in bacteria. Nat Microbiol 9:2395–2409.

41. Das S, Forrest J, Kuzminov A. 2023. Synthetic lethal mutants in *Escherichia coli* define pathways necessary for survival with RNase H deficiency. J Bacteriol 205:e0028023.

42. Keseler IM, Gama-Castro S, Mackie A, Billington R, Bonavides-Martínez C, Caspi R, Kothari A, Krummenacker M, Midford PE, Muñiz-Rascado L, Ong WK, Paley S, Santos-Zavaleta A, Subhraveti P, Tierrafría VH, Wolfe AJ, Collado-Vides J, Paulsen IT, Karp PD. 2021. The EcoCyc Database in 2021. Front Microbiol 12:711077.

43. Sayers EW, Beck J, Bolton EE, Bourexis D, Brister JR, Canese K, Comeau DC, Funk K, Kim S, Klimke W, Marchler-Bauer A, Landrum M, Lathrop S, Lu Z, Madden TL, O'Leary N, Phan L, Rangwala SH, Schneider VA, Skripchenko Y, Wang J, Ye J, Trawick BW, Pruitt KD, Sherry ST. 2021. Database resources of the National Center for Biotechnology Information. Nucleic Acids Res 49:D10–D17.

44. Mitchener MM, Begley TJ, Dedon PC. 2023. Molecular Coping Mechanisms: Reprogramming tRNAs To Regulate Codon-Biased Translation of Stress Response Proteins. Acc Chem Res 56:3504–3514.

45. Baba T, Ara T, Hasegawa M, Takai Y, Okumura Y, Baba M, Datsenko KA, Tomita M, Wanner BL, Mori H. 2006. Construction of *Escherichia coli* K□12 in□frame, single□gene knockout mutants: the Keio collection. Mol Syst Biol 2:2006.0008.

46. Typas A, Nichols RJ, Siegele DA, Shales M, Collins SR, Lim B, Braberg H, Yamamoto N, Takeuchi R, Wanner BL, Mori H, Weissman JS, Krogan NJ, Gross CA. 2008. A tool-kit for high-throughput, quantitative analyses of genetic interactions in *E. coli*. Nat Methods 5:781.

47. Datsenko KA, Wanner BL. 2000. One-step inactivation of chromosomal genes in *Escherichia coli* K-12 using PCR products. Proc Natl Acad Sci U S A 97:6640.

48. McClain WH, Gabriel K, Lee D, Otten S. 2004. Structure–function analysis of tRNAGln in an *Escherichia coli* knockout strain. RNA 10:795.

49. Bertani G. 1951. STUDIES ON LYSOGENESIS I.□: The Mode of Phage Liberation by Lysogenic *Escherichia coli*. J Bacteriol 62:293.

50. Moore SD. 2011. Assembling new *Escherichia coli* strains by transduction using phage P1. Methods Mol Biol 765:155–169.

51. Björk GR, Hagervall TG. 2005. Transfer RNA modification, p. http://www.ecosal.org. *In* Böck, A, Curtis, R, Kaper, JB, Neidhardt, FC, Nyström, T, Squires, CL (eds.), *Escherichia coli* and Salmonella. Cellular and Molecular Biology. ASM. Press, Washington DC.

52. Sakai Y, Kimura S, Suzuki T. 2019. Dual pathways of tRNA hydroxylation ensure efficient translation by expanding decoding capability. Nat Commun 10:2858.

53. Nilsson K, Jäger G, Björk GR. 2017. An unmodified wobble uridine in tRNAs specific for Glutamine, Lysine, and Glutamic acid from Salmonella enterica Serovar Typhimurium results in nonviability-Due to increased missense errors? PLoS One 12:e0175092–e0175092.

Figure 1

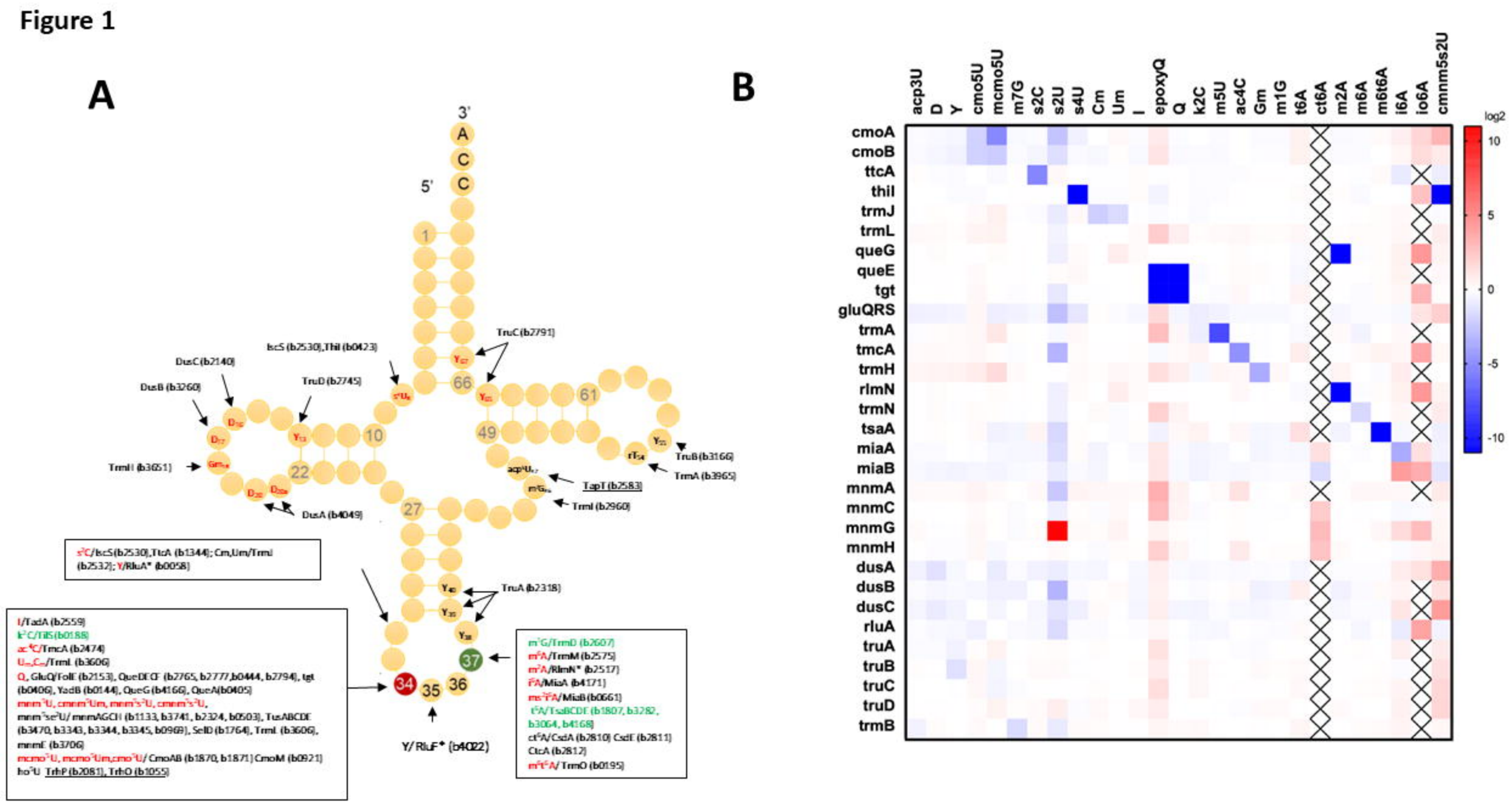
A
B
3'
5'
A
C
C
1
10
22
27
34
35
36
37
49
61
66
TrmI (b3651)
DusA (b4049)
DusB (b3260)
DusC (b2140)
IscS (b2530),TilI (b0423)
TruD (b2745)
TruC (b2791)
TrmA (b3965)
TruB (b3166)
TapT (b2583)
TrmI (b2960)
TruA (b2318)
s2C/IscS(b2530),TtcA (b1344); Cm,Um/TrmJ (b2532); Y/RluA* (b0058)
I/TadA (b2559)
k2C/TilS (b0188)
ac4C/TmcA (b2474)
U34,C34/TrmL (b3606)
Q, GluQ/FolE (b2153), QueDEC1C2 (b2765, b2777,b0444, b2794), tgt (b0406), YadB (b0144), QueG (b4166), QueA(b0405)
mnm5U, cmnm5Um, mnm5s2U, cmnm5s2U, mnm5se2U/ mnmAGCH (b1133, b3741, b2324, b0503), TusABCDE (b3470, b3343, b3344, b3345, b0969), SelD (b1764), TrmL (b3606), mnmE (b3706)
mcmo5U, mcmo5Um,cmo5U/ CmoAB (b1870, b1871) CmoM (b0921)
ho5U TrhP (b2081), TrhO (b1055)
Y/RluF* (b4022)
m1G/TrmD (b2607)
m1A/TrmM (b2575)
m2A/RlmN* (b2517)
i6A/MiaA (b4171)
ms2i6A/MiaB (b0661)
t6A/TsaBCDE (b1807, b3282, b3064, b4168)
ct6A/CsdA (b2810) CsdE (b2811) CtcA (b2812)
m6t6A/TrmO (b0195)
acp3U
D
Y
cmo5U
mcmo5U
m7G
s2C
s2U
s4U
Cm
Um
I
epoxyQ
Q
k2C
m5U
ac4C
Gm
m1G
t6A
ct6A
m2A
m6A
m6t6A
i6A
io6A
cmnm5s2U
cmoA
cmoB
ttcA
thiI
trmJ
trmL
queG
queE
tgt
gluQRS
trmA
tmcA
trmH
rlmN
trmN
tsaA
miaA
miaB
mnmA
mnmC
mnmG
mnmH
dusA
dusB
dusC
rluA
truA
truB
truC
truD
trmB
log2
10
5
0
-5
-10

Figure 2

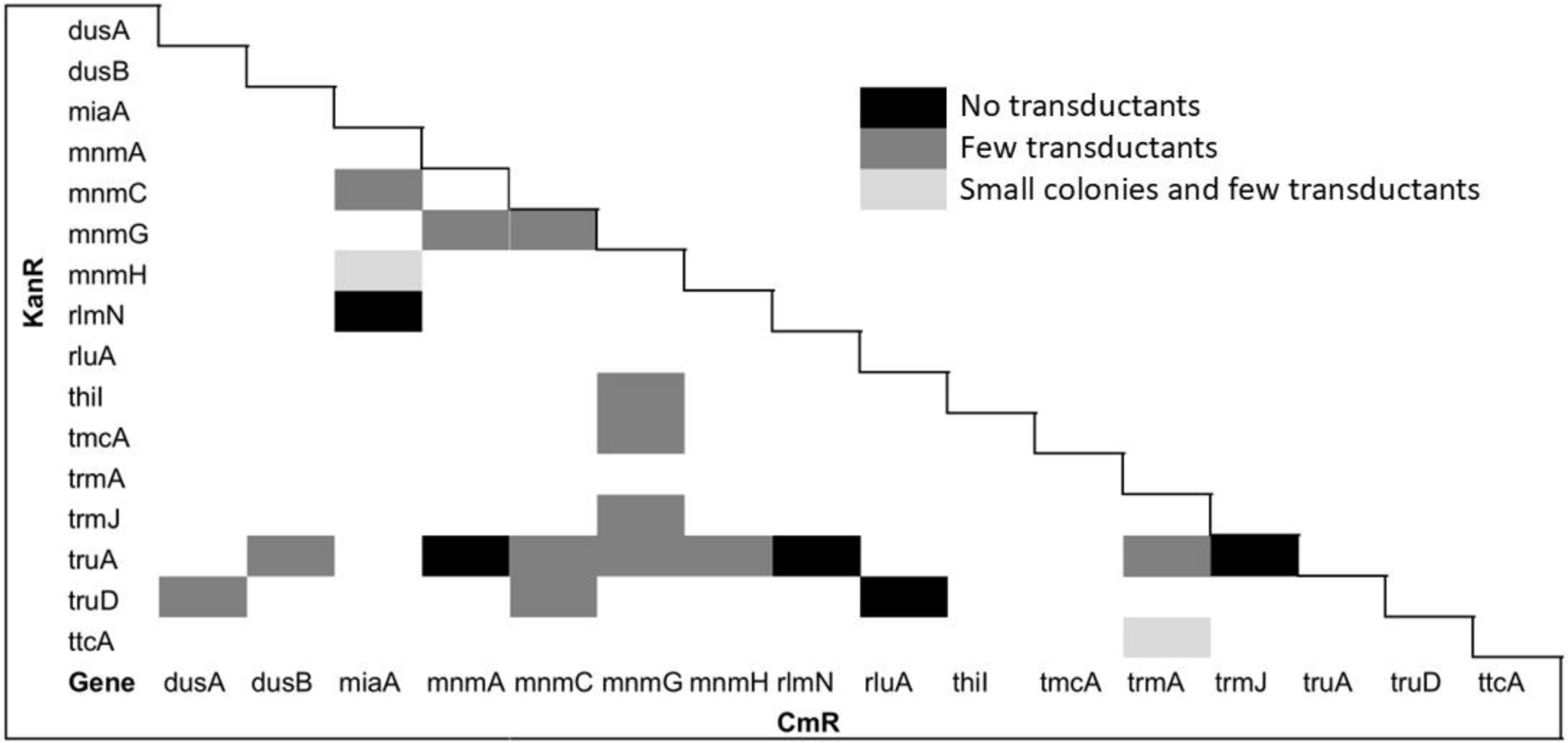
No transductants
Few transductants
Small colonies and few transductants
KanR
dusA
dusB
miaA
mnmA
mnmC
mnmG
mnmH
rlmN
rluA
thiI
tmcA
trmA
trmJ
truA
truD
ttcA
Gene
dusA dusB miaA mnmA mnmC mnmG mnmH rlmN rluA thiI tmcA trmA trmJ truA truD ttcA
CmR

Figure 3

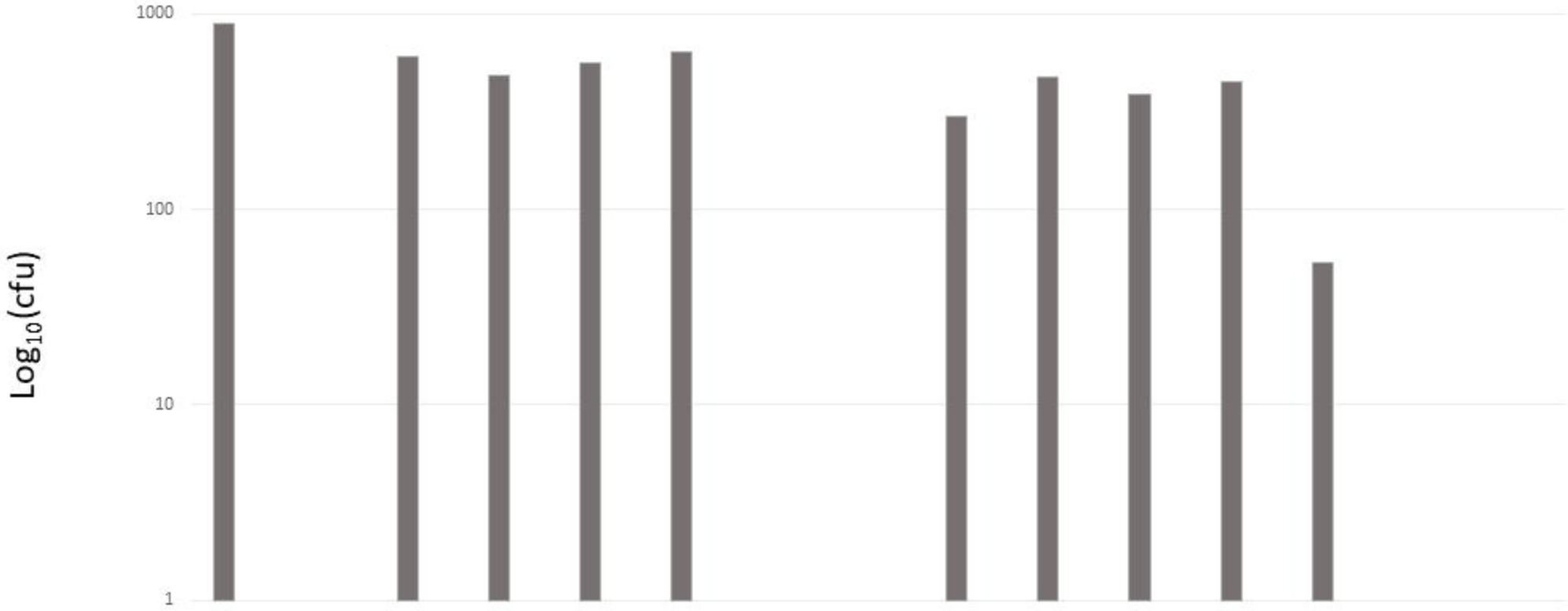

Strain	WT	*ΔtruA*	WT	WT	WT	WT	*ΔtruA*	*ΔtruA*	*ΔtruA*	*ΔtruA*	WT	WT	*ΔtruA*	*ΔtruA*
Vector	-	-	pBAD24	pBAD24	pTruA	pTruA	pBAD24	pBAD24	pTruA	pTruA	pGln1	pGln2	pGln1	pGLn2
Ara	-	-	-	+	-	+	-	+	-	+	-	-	-	-
IPTG	-	-	-	-	-	-	-	-	-	-	+	+	+	+

Figure 4

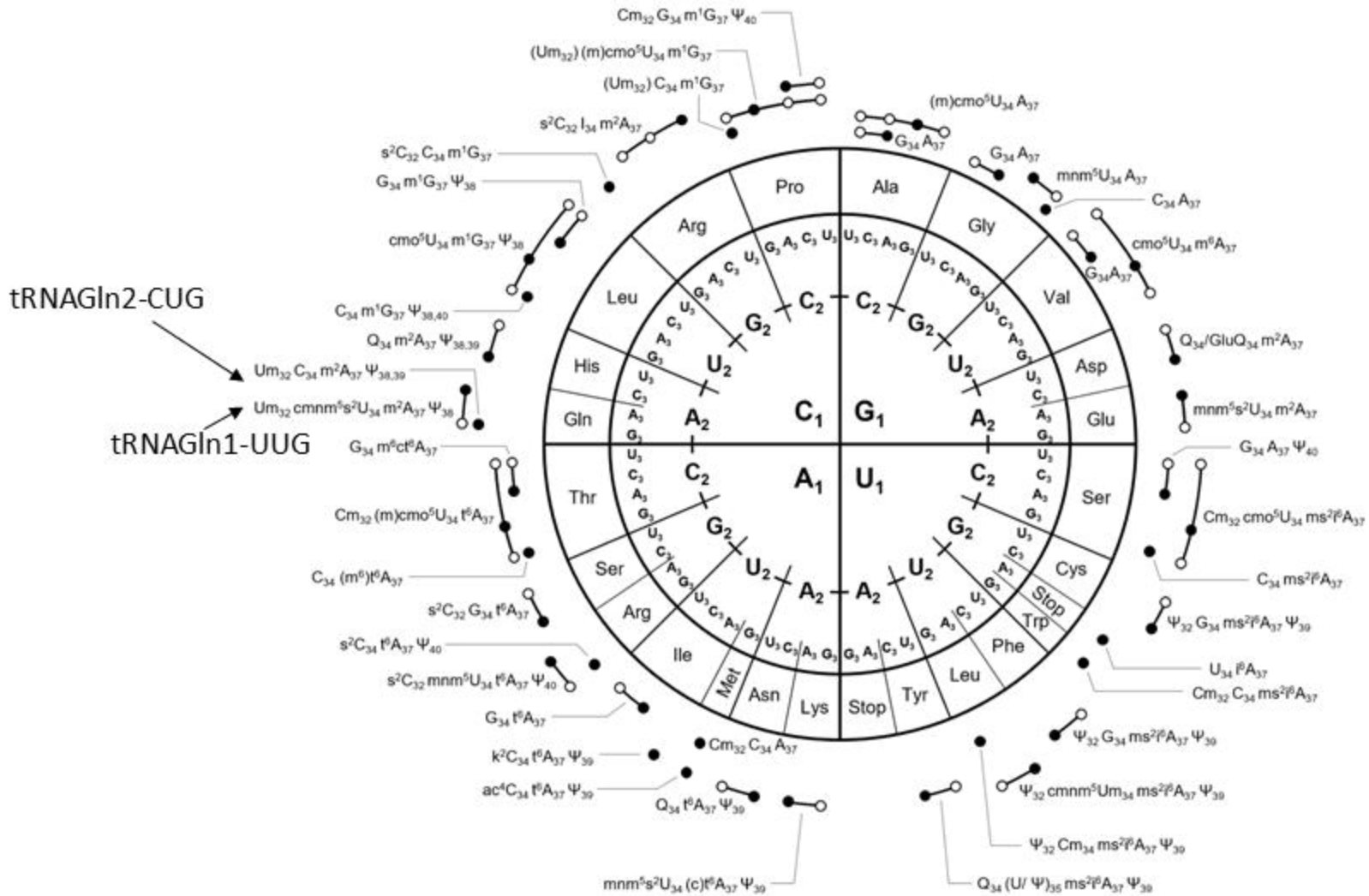
tRNAGln2-CUG
tRNAGln1-UUG
Cm32 G34 m1G37 Ψ40
(Um32) (m)cmo5U34 m1G37
(Um32) C34 m1G37
s2C32 I34 m2A37
s2C32 C34 m1G37
G34 m1G37 Ψ38
cmo5U34 m1G37 Ψ38
C34 m1G37 Ψ38,40
Q34 m2A37 Ψ38,39
Um32 C34 m2A37 Ψ38,39
Um32 cmnm5s2U34 m2A37 Ψ38
G34 m6ct6A37
Cm32 (m)cmo5U34 t6A37
C34 (m6)t6A37
s2C32 G34 t6A37
s2C34 t6A37 Ψ40
s2C32 mnm5U34 t6A37 Ψ40
G34 t6A37
k2C34 t6A37 Ψ39
ac4C34 t6A37 Ψ39
Q34 t6A37 Ψ39
mnm5s2U34 (c)t6A37 Ψ39
Cm32 C34 A37
(m)cmo5U34 A37
G34 A37
G34 A37
mnm5U34 A37
C34 A37
cmo5U34 m6A37
G34A37
Q34/GluQ34 m2A37
mnm5s2U34 m2A37
G34 A37 Ψ40
Cm32 cmo5U34 ms2i6A37
C34 ms2i6A37
Ψ32 G34 ms2i6A37 Ψ39
U34 i6A37
Cm32 C34 ms2i6A37
Ψ32 G34 ms2i6A37 Ψ39
Ψ32 cmnm5Um34 ms2i6A37 Ψ39
Ψ32 Cm34 ms2i6A37 Ψ39
Q34 (U/ Ψ)35 ms2i6A37 Ψ39
Pro
Ala
Gly
Val
Asp
Glu
Ser
Cys
Stop
Trp
Phe
Leu
Tyr
Stop
Lys
Asn
Met
Ile
Arg
Ser
Thr
Gln
His
Leu
Arg
C1
G1
A1
U1
C2
G2
U2
A2

Figure 5

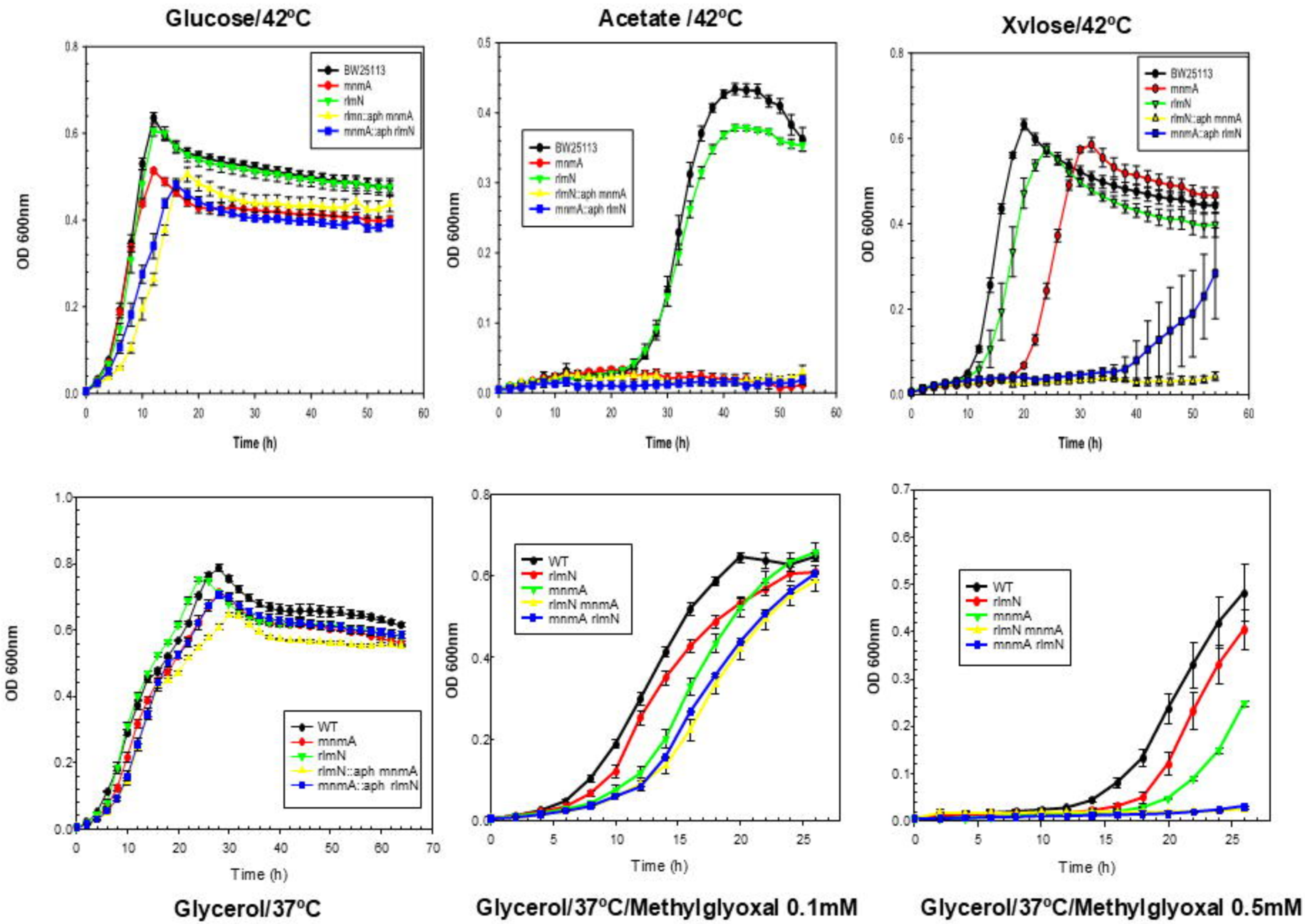
Glucose/42°C
Acetate /42°C
Xylose/42°C
BW25113
mnmA
rlmN
rlmN::aph mnmA
mnmA::aph rlmN
OD 600nm
Time (h)
WT
Glycerol/37°C
Glycerol/37°C/Methylglyoxal 0.1mM
Glycerol/37°C/Methylglyoxal 0.5mM